Positron motion in metals. III. Effects of positron interactions with electrons and phonons

T. Hyodo,* T. McMullen, and A. T. Stewart
Department of Physics, Queen's University, Kingston, Ontario, Canada K7L 3N6
(Received 8 July 1985)

High-precision, high-resolution measurements of the angular correlation of annihilation radiation from potassium single crystals are reported. These data yield information on the interactions of positrons with electrons and phonons. The momentum dependence of the annihilation rate appears to be larger than recent theoretical predictions. The positron quasiparticle mass in potassium, free from the apparent mass enhancement due to phonon scattering, is found to be $m^*=(1.4\pm0.1)m_e$. The positron-phonon coupling strength is also obtained.

I. INTRODUCTION

The positron is a unique probe of many-body interactions in matter. A close examination of the 511-keV photons from its annihilation can reveal the details of interactions which have characteristic energies of well below 300 K.

The positron is shot into condensed matter—usually from a radioactive nucleus. It loses energy rapidly and is usually long thermalized before annihilating in about 10^{-10} s. In a metal the thermalized positron collects around itself a polarization cloud of electrons in which it annihilates. The electron density at the positron is one many-body effect that is directly measured in the lifetime of the positron. The reciprocal of the lifetime, the annihilation rate, shows that the electron density at the positron is several times the local density in the unperturbed host metal. By and large the observed annihilation rates and the enhanced charge density calculated in many-body theories agree quite well.[1]

A more subtle many-body effect is observable in the total momentum of the annihilation γ rays and hence of the electron-positron pair at the instant of annihilation. The "longitudinal" component of this momentum can be measured (but not with very high resolution) by the Doppler shift of the γ-ray energy; while the "transverse" component of momentum can be measured (to high precision) in the departure of the two annihilation photons from collinearity. (The departure from 180° is very small: $\theta\simeq 2mv/mc\simeq$a few milliradians (mrad) with v the center-of-mass velocity of the annihilating pair and mc^2 the electron rest energy.) Careful measurements of the angular correlation of annihilation γ rays have been shown that electrons near the Fermi surface are somewhat more likely to annihilate than those of lower energy. This momentum dependence of electron density in the polarization cloud can be both measured and calculated—with difficulty. Unfortunately, at present even the theories do not agree and as this paper will show, the experimental data, although favoring one, does lie between.

The motion of the positron itself can also be observed. The angular distribution of the annihilation photons shows a sharp cutoff at the maximum momentum, the Fermi momentum p_F, for free-electron-like metals. As Bergersen and Pajanne[2] have shown, the momentum distribution of annihilating electron-positron pairs may be approximated as the convolution of the single-particle momentum distributions. At the discontinuity of the electron distribution, i.e., at the Fermi momentum, the observation reveals directly the momentum distribution of the positron. With sufficiently high experimental resolution the "smearing" of the cutoff at p_F can be measured and the motion of the positron deduced. This observed motion reveals the effective mass of the positron due to electron interactions, and the effect of phonons on the positron dynamics.

Experimentally, the smearing has been characterized by a Boltzmann distribution of the positron momentum.[3–5] The experimental values for the mass parameter characterizing the distribution, customarily called the effective mass, were larger than the theoretically calculated positron effective mass including band[4,6–8] and positron-electron[9–11] interaction effects only. Mikeska[12,13] and Bergersen and Pajanne[2] showed that the positron-phonon interaction is important, and that it not only makes the positron momentum distribution wider than it would be without phonons, but it also adds a tail to the distribution which asymptotically decreases as p^{-4}. This non-Gaussian shape was believed to be responsible for the additional smearing of the Fermi cutoff.

Recently, Kubica and Stewart (Ref. 14, hereafter referred to as I) measured the angular correlation of annihilation radiation from simple metals. They analyzed the data with a Gaussian positron momentum distribution and interpreted the fitted width parameter as an "apparent mass," thereby attempting to include the effect of the positron-phonon scattering. This Gaussian fit to the experimental data is in fair agreement with a similar Gaussian fit to the theory by Bergersen and Pajanne.[2]

However, in the presence of the high momentum tail, the apparent mass appears not to be a good physical parameter; it has only an approximate meaning. In fact, the data of I appear to suggest that the apparent mass is temperature dependent. In recent papers by the present authors (Refs. 5, 15, and 16, the last referred to hereafter as

II) the meaning of the apparent mass approximation is clarified. It is emphasized in II that the effect of the p^{-4} tail cannot be fully accounted for by the Gaussian approximation. As an alternative, it was proposed in II that the realistic distribution should be used in the analysis, which then allows one to separate the quasiparticle mass of the positron and the (renormalized) positron-phonon coupling constant.

The experiment reported in the present paper was designed to determine these quantities by observing the thermal smearing of the angular correlation of radiation from positron annihilation in potassium single crystals. Very high experimental resolution was used, and special care was taken in determining the actual shape of the resolution function. Statistical precision of more than 10 000 counts per point around the Fermi cutoff was attained. The method of analysis, discussed in detail in II, does not depend crucially on the shape of the background which is composed[17] of the contributions from annihilations with core electrons and from the higher momentum components of the wave functions of the conduction electrons and the positron. This feature is highly advantageous when one analyzes detailed structure of the smearing. This method also leads us to a reliable estimate of the momentum dependence of the annihilation rate.

The next section gives the theoretical background of the present experiment. Experimental arrangements are described in Sec. III. The analysis is shown in Sec. IV, and the results[18] are discussed in Sec. V. A summary is given in the last section.

II. THEORETICAL BACKGROUND

A. Positron-electron interaction

The positron-electron interaction has several effects[19] on the annihilation. It causes enhancement of the annihilation rate due to the increase in electron density at the position of the positron. This enhancement is momentum dependent, which makes the long slit projection of the momentum distribution of the annihilating pair a "bulgy" parabola.[20,21] The positron-electron interaction also gives a contribution to the positron effective mass m^*. In addition, the interaction renormalizes the positron-phonon coupling by the quasiparticle renormalization constant Z_0.

There are basically three kinds[22] of theoretical calculations of the momentum-dependent enhancement $\epsilon(p)$. The first was the work of Kahana[23] and its extensions.[20,24–27] Kahana recognized that the positron-electron interaction was strong enough to prohibit the use of any linear screening theory, and proposed that multiple scattering of the electron from the positron be included by a ladder sum using the static limit of the random-phase-approximation (RPA) interaction. The total annihilation rate calculated in this way unfortunately diverges[28] for $r_s > 6$, and so is presumably unsuitable, as it stands, for the low electron density metals, such as K with $r_s = 4.86$.

The second class of calculation is that of Arponen and Pajanne.[29] They use a boson model of the interacting electron gas in which the elementary excitations (of the RPA) are represented by an appropriate boson spectrum with residual interactions. The total rate calculated in this way is well behaved in the low-density limit,[1] and the momentum dependence of $\epsilon(p)$ is appreciably less than in the Kahana theory.

The third style of calculation is that of Lowy.[30] It is based on an effective interaction which includes nonlinear screening effects from only one highly correlated electron at any one time. The momentum dependence of $\epsilon(p)$ which results from this calculation is intermediate between that of Kahana and that of Arponen and Pajanne.

The positron-electron interaction also increases the positron quasiparticle effective mass m^* over the bare mass m_e. RPA-based calculations exist for the effective mass of positrons in an electron gas corresponding to the electron density of potassium metal. (It should, however, be recalled that RPA calculations of the annihilation rate at this density give a rate which is much too small.) Hamann[9] finds $m^* = 1.18 m_e$ in a straightforward RPA self-energy calculation. Baldo and Pucci[11] included a vertex correction as well, and obtained $m^* = 1.43 m_e$. The reference mass should more properly be the positron band mass m_b rather than the bare mass m_e. This has been calculated for potassium by Stott and Kubica[7] as $m_b = 1.11 m_e$ using the positron pseudopotential technique, and by Fletcher *et al.*[8] as $m_b = 1.06 m_e$ using the electron band-structure calculations by Moruzzi *et al.*[31]

The remaining effect of the positron-electron interaction is to fix the quasiparticle renormalization constant Z_0. The only calculations for potassium are those of Baldo and Pucci[11] for the electron gas giving $Z_0 = 0.38$, and Mori's calculation[32] for the liquid state giving $Z_0 = 0.64$. Z_0 as well as m^* enters the renormalization of the positron-phonon coupling to be described in the following section.

B. Positron-phonon interaction

The positron-phonon interaction has its most noticeable effect on the angular correlation spectrum in the vicinity of the Fermi cutoff, where a temperature-dependent smearing of the sharp cutoff can be seen. Smearing is expected even in an independent-particle model, of course, because the positron acquires nonzero thermal momentum. However, the observed smearing is greater than that resulting from the thermal motion of a free particle of mass m^*. This observation led to the analysis of the thermal smearing by Mikeska[12,13] and by Bergersen and Pajanne.[2] The analysis is subtle, and the underlying physical concepts have not always been fully appreciated. It is the presence of two interactions, the positron-electron interaction as well as the positron-phonon interaction, that tends to obscure the essentially simple physical phenomena. However, the positron-electron interaction does not play a very significant role in the thermal smearing problem. As shown by Bergersen and Pajanne, it simply renormalizes the mass and positron-phonon coupling constant. In contrast, it is all important in the annihilation rate enhancement, where the positron-phonon interaction has a negligible effect.

A derivation of thermal smearing which ignores the positron-electron interaction is illuminating, for it is appreciably simpler than the argument required for the complete problem, and yet it contains the essential physical ideas. The result obtained can be converted to that for the complete problem by merely replacing the mass and coupling constant by their renormalized values. We present such a derivation here, in the hope that the reader will find it helpful. For a proper derivation of thermal smearing in the full problem including the positron-electron interaction the interested reader is referred to the fundamental paper of Bergersen and Pajanne.[2]

The probability of a 2γ annihilation with total momentum $\mathbf{K}$ is

$$P(\mathbf{K}) \propto \sum_{\mathbf{k}\mathbf{k}'} \langle c_{\mathbf{k}}^{\dagger} b_{\mathbf{K}-\mathbf{k}}^{\dagger} b_{\mathbf{K}-\mathbf{k}'} c_{\mathbf{k}'} \rangle , \tag{1}$$

where c_k annihilates a positron and b_k annihilates an electron, and $\langle \cdots \rangle$ represents a trace over the equilibrium density matrix. Spin indices have been suppressed. Suppose that the positron interacts only with phonons, not with electrons, as described by the Hamiltonian $H=H^0+H'$ with

$$H^0=\sum_{\mathbf{k}} \epsilon_{\mathbf{k}} c_{\mathbf{k}}^{\dagger} c_{\mathbf{k}}^{\dagger} + \sum_{\mathbf{q}\lambda} \omega_{\mathbf{q}\lambda} a_{\mathbf{q}\lambda}^{\dagger} a_{\mathbf{q}\lambda} \tag{2}$$

the noninteracting system, and

$$H'=\sum_{\mathbf{k}\mathbf{q}\lambda} g_{\mathbf{q}\lambda} c_{\mathbf{k}+\mathbf{q}}^{\dagger} c_{\mathbf{k}} \phi_{\mathbf{q}\lambda} , \tag{3}$$

where $\phi_{\mathbf{q}\lambda}=a_{\mathbf{q}\lambda}+a_{-\mathbf{q}\lambda}^{\dagger}$ ($\hbar=1$ throughout this section). The operator $a_{\mathbf{q}\lambda}$ annihilates a phonon of wave vector $\mathbf{q}$, polarization λ, and frequency $\omega_{\mathbf{q}\lambda}$, and $g_{\mathbf{q}\lambda}$ gives the positron-phonon coupling. Then the expectation value in (1) becomes a convolution

$$P(\mathbf{K}) \propto \sum_{\mathbf{k}} \langle b_{\mathbf{K}-\mathbf{k}}^{\dagger} b_{\mathbf{K}-\mathbf{k}} \rangle F(\mathbf{k}) , \tag{4}$$

where

$$F(\mathbf{k})=\langle c_{\mathbf{k}}^{\dagger} c_{\mathbf{k}} \rangle \tag{5}$$

is the positron momentum distribution. $F(\mathbf{k})$ is conveniently written as a limit

$$F(\mathbf{k})=\lim_{t\to 0_-} G_{\mathbf{k}}(t) \tag{6}$$

of the finite temperature Green function[33]

$$G_{\mathbf{k}}(t)=-\langle \mathcal{T} c_{\mathbf{k}}(t) c_{\mathbf{k}}^{\dagger} \rangle . \tag{7}$$

It is useful to rewrite (6) using the Fourier series

$$G_k(t)=\frac{1}{\beta}\sum_{\omega_n} e^{-i\omega_n t} G_{\mathbf{k}}(i\omega_n) \tag{8}$$

with $\beta^{-1}=k_B T$ and $\omega_n=(2n+1)\pi/\beta$, $n=0,\pm 1,\ldots$. The positron self-energy $\Sigma_{\mathbf{k}}(i\omega_n)$ and spectral function $\rho_{\mathbf{k}}(\omega)$ are introduced by writing

$$G_k(i\omega_n)=[i\omega_n-\epsilon_{\mathbf{k}}-\Sigma_{\mathbf{k}}(i\omega_n)+\mu]^{-1} , \tag{9}$$

and

$$\rho_{\mathbf{k}}(\omega)=2\,\mathrm{Im} G_{\mathbf{k}}(\omega-i\eta) . \tag{10}$$

With use of these definitions,

$$F(\mathbf{k})=\int_{-\infty}^{\infty} \frac{d\omega}{2\pi} \frac{\rho_{\mathbf{k}}(\omega)}{1+e^{\beta\omega}} , \tag{11}$$

showing that the positron momentum distribution is a weighted average over the spectral function, with the weighting function essentially a Boltzmann factor since $\rho_{\mathbf{k}}(\omega)$ is peaked near $\omega=\epsilon_k-\mu$. The normalization $\sum_{\mathbf{k}} F(\mathbf{k})=1$ shows that μ is large and negative in the limit of low positron density.

The positron-phonon self-energy is believed[34] to be adequately approximated by the single diagram shown in Fig. 1, which gives

$$\Sigma_{\mathbf{k}}(\omega-i\eta)=\sum_{\mathbf{q}\lambda} |g_{\mathbf{q}\lambda}|^2 \frac{1}{\bar{\omega}-i\eta-\epsilon_{\mathbf{k}-\mathbf{q}}+\omega_{\mathbf{q}\lambda}} \frac{1}{e^{\beta\omega_{\mathbf{q}\lambda}}-1} + \frac{1}{\bar{\omega}-i\eta-\epsilon_{\mathbf{k}-\mathbf{q}}-\omega_{\mathbf{q}\lambda}} \frac{1}{1-e^{\beta\omega_{\mathbf{q}\lambda}-1}} , \tag{12}$$

where, for coupling to longitudinal acoustic phonons with $\omega_q=sq$,

$$|g_q|^2=\frac{\pi^2\chi}{\Omega}\frac{E_F}{k_F^3}\omega_q \tag{13}$$

with $k_F=(9\pi/4)^{1/3} r_s^{-1}$, the electron-gas–model Fermi wave vector, and $E_F=k_F^2/2m_e$, the corresponding Fermi energy. We have introduced $\bar{\omega}=\omega+\mu$, Ω is the volume, and the coupling constant

$$\chi=(3s_0 D/2sE_F)^2 \tag{14}$$

measures the difference of the deformation potential D from $-2E_F/3$ and of the sound velocity from the Bohm-Staver value[35] s_0. When $\Sigma_{\mathbf{k}}(\omega-i\eta)=\Delta_{\mathbf{k}}(\omega)+i\Gamma_{\mathbf{k}}(\omega)$ is separated into real and imaginary parts, the real part $\Delta_{\mathbf{k}}$ is found to be negligibly small.[13,36] It is the imaginary part

$$\Gamma_{\mathbf{k}}(\omega)=\frac{\pi\chi}{2\beta}(m^*/m_e)^{3/2}\left[\frac{\bar{\omega}}{E_F}\right]^{1/2}\Theta(\bar{\omega}) \tag{15}$$

that causes thermal smearing of the momentum distribution, where Θ is the unit step function. Since $\Gamma_{\mathbf{k}}$ is closely related to the positron-phonon scattering rate, this smearing is best regarded as an uncertainty principle broadening.

On neglecting the real part $\Delta_{\mathbf{k}}$ of the self-energy the spectral function becomes

$$\rho_{\mathbf{k}}(\omega)=\frac{2\Gamma_{\mathbf{k}}(\omega)}{(\bar{\omega}-\epsilon_{\mathbf{k}})^2+[\Gamma_{\mathbf{k}}(\omega)]^2} . \tag{16}$$

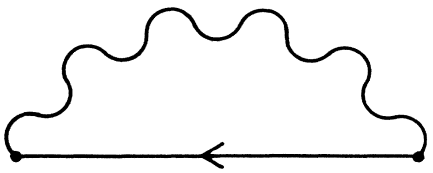

FIG. 1. Lowest-order contribution to the positron-phonon self-energy $\Sigma_{\mathbf{k}}(\omega)$.

Since $\Gamma_k(\omega) \propto (\bar{\omega})^{1/2}$, (16) is not a simple Lorentzian. A figure showing the k and ω dependence of $\rho_k(\omega)$ can be found in Ref. 37. Bergersen and Pajanne[2] show that when the positron-electron interaction is properly included, expression (16) is modified in two ways: The coupling constant χ is replaced by its renormalized value $\tilde{\chi}=Z_0\chi$, where Z_0 is the quasiparticle renormalization constant, and m^* is not just the band mass m_b but includes the positron-electron mass enhancement as well. In addition, (16) is multiplied by an overall factor Z_0. Since there is some cancellation between the renormalization of χ and the renormalization of the mass, both must be included (or, for an approximate result, both should be omitted).

III. EXPERIMENT

A long slit angular correlation apparatus was used for the measurement. Potassium single crystals were oriented so that the projection of the momentum on the [110] or [100] direction was measured. The specimens were spark cut cylinders of about 8 mm in diameter and about 5 mm in length. The error in orientation was estimated to be $\pm 1°$. The top surface of each specimen was cut at an angle $\approx 4°$ to the (110) or (100) plane of the crystal to avoid possible asymmetry of the data due to the variation in the absorption of γ rays. The effective positron penetration profile of each specimen was measured by scanning a very fine (0.1 mm) slit close to the sample chamber, and was used to calculate the actual resolution function used in the analysis of data for each specimen. The slanted specimen surface also served to make the profile and hence the resolution function more symmetrical. The full width at half maximum of the resolution function was about 0.20 mrad ($0.20\times10^{-3}mc$) for the measurement at 298 and 199 K and about 0.15 mrad for those at 91 K.

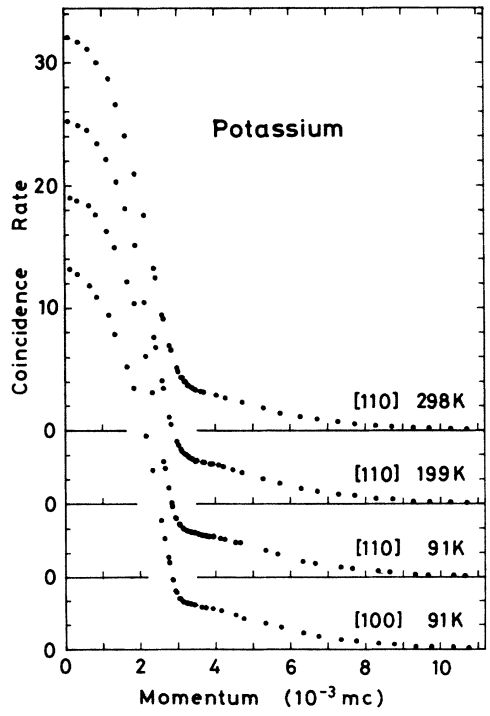

FIG. 2. Long slit projections onto the [110] and [100] directions of the momentum distribution of photon pairs from positrons annihilating with electrons in potassium single crystals at the temperatures indicated.

The sample chamber was a small In sealed glass jar so that one could see the specimen surface *in situ*. The formation of thin oxide film was observed in about one day after the specimen was mounted even though the chamber was continuously pumped by a diffusion pump. However, there seemed to be no further appreciable change after that when the seal was perfect. In fact, the data obtained in the first half of the measurement at each temperature showed no difference above statistical fluctuations for those in the last half.

The observed data are shown in Fig. 2 after normalization to the same area. the number of coincidence counts per point near the Fermi cutoff for the data along [110] was more than 10000 (100000—140000 at the center), while the number for the data along [100] was about 8000 (about 60000 at the center).

IV. ANALYSIS OF DATA

The data shown in Fig. 2 consist of several contributions: the central part due to conduction electrons, the core electron contribution, contributions from higher momentum components of the positron and electron wave functions, and the smearing around p_F due to the positron momentum distribution. None of these is known well enough to calculate and subtract in order to apply ordinary least-squares analysis. The new analysis proposed in II, which allows separation of the positron quasiparticle mass from the phonon scattering effect, was invented in the hope of avoiding this difficulty. The method starts by constructing the central part. Neglecting the small p dependence of intensity due to the lattice, the spherical Fermi surface yields a parabolic shape. This parabola is modified by the isotropic enhancement factor,

$$\epsilon(p)=a\left[1+(b/a)(p/p_F)^2+(c/a)(p/p_F)^4\right], \qquad (17)$$

and convoluted with the positron momentum distribution [Eqs. (11) and (16)] and the experimental resolution function. Then, each of the possible shapes is subtracted from the data and the remainder is examined to determine if it agrees with reasonable assumptions for the shape of the core and the high momentum components.

The structure and intensity of the data outside the Fermi cutoff helps us to make a better guess of these components. Figure 3 shows the expanded portion of the data along [110] around and outside the Fermi cutoff. It is seen that these data have a characteristic structure common for different temperatures, but that the intensity depends on temperature. The structure, best seen at 91 K, is closely related to the edge of the projection on the [110] direction of a Fermi sphere centered at each (110) reciprocal-lattice point as shown in Fig. 4. This indicates that the higher momentum components do exist and that geometry determines to a considerable extent the shape of the contribution. When this analysis was started, little was known about the higher momentum components and so we tried various hypothetical functions for the intensity

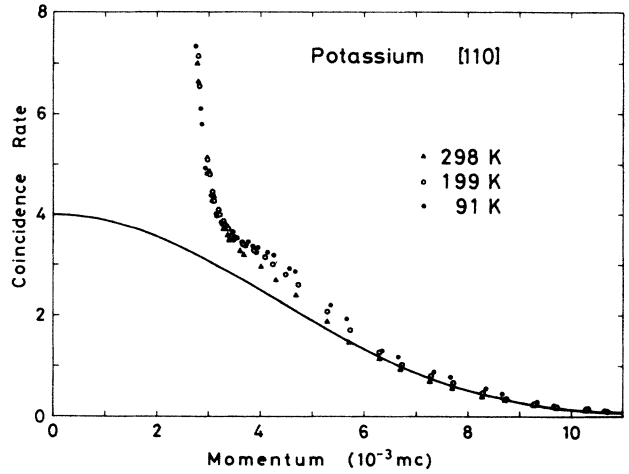

FIG. 3. Expanded portion of the data along [110] in Fig. 2. The solid line shows the experimentally observed momentum distribution for argon with an intensity suitable for an estimate of the core contribution to the data at 91 K.

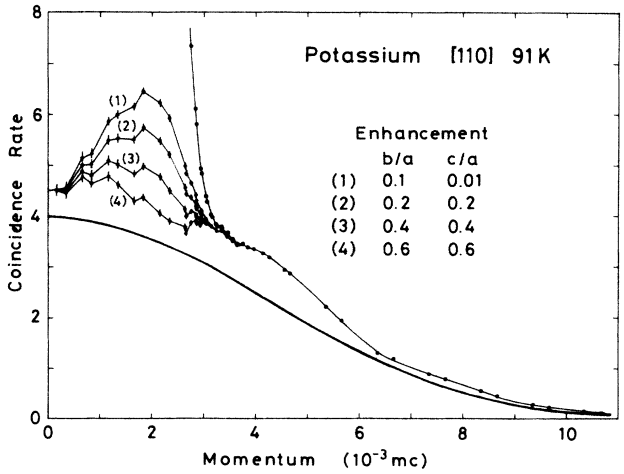

FIG. 5. An expanded portion of the data along the [110] direction at 91 K. The curves (1)—(4) are examples of the remainder after the parabolic part with various enhancement factors was subtracted from the data. Other parameters are fixed at $p_F=2.87\times10^{-3}mc$, $m^*=1.4$, and $\tilde{\chi}=1.3$.

of the (110) higher momentum component. These functions supposed that the intensity was determined only by the distance from the zone boundary. The resultant higher momentum intensities projected onto the [110] axis are shown in Fig. 4. As noted above, most of the structure of the projected components comes from geometry, not from the particular functional form hypothesized. It should be noted that "trial functions" numbers 2,3,4 fitted about equally well. Recently, the higher momentum components have been measured directly. (A preliminary report is given by Oberli *et al.*,[38] and a full report will be submitted for publication.) These direct measurements agree well with our hypothesized forms in magnitude and in structure, thus confirming the validity of this analysis. Comparing the observed structure for $k>k_F$ with model predictions enabled us to estimate the relative weights of the core and the high momentum components. Using the same relative weights, the [100] projection was then constructed and tested against observed data as a check for self-consistency.

The best assumption at present for the shape of the core contribution seems to be the experimentally observed momentum distribution for positron annihilation in solid argon. This is shown in Fig. 3 drawn with the intensity assumed for the data at 91 K. It is obvious that the same curve cannot be regarded as the core contribution for the data at higher temperatures. Curves of somewhat narrower width and lower intensity were assumed for higher temperatures, with the choice guided by the intensity of the structure in the data outside the Fermi cutoff. The

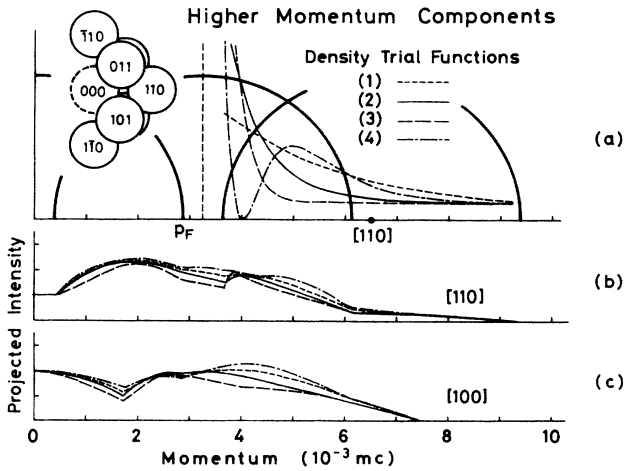

FIG. 4. Long slit projection onto the (b) [110] and (c) [100] directions of (110) higher momentum components with various hypothetical momentum density functions (a). Large semicircles in (a) indicate the projections of the Fermi sphere centered at each (110) reciprocal-lattice point [inset in (a)] onto the [110] direction.

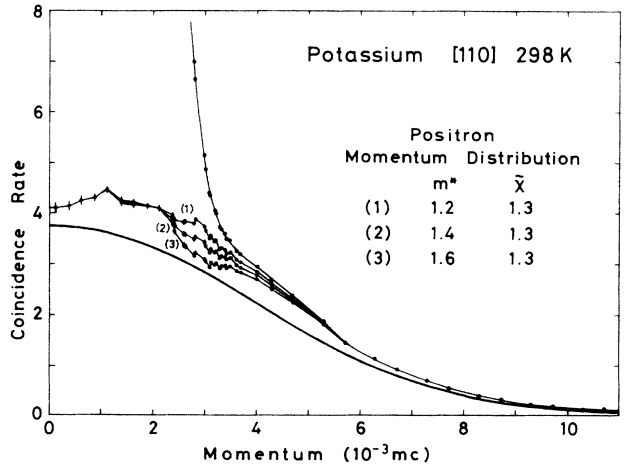

FIG. 6. An expanded portion of the data along the [110] direction at 298 K. The curves (1)—(3) are examples of the remainder after the parabolic part with various smearing functions was subtracted from the data. The value of $\tilde{\chi}$ is fixed, as is $p_F=2.81\times10^{-3}mc$ and $b/c=c/a=0.35$.

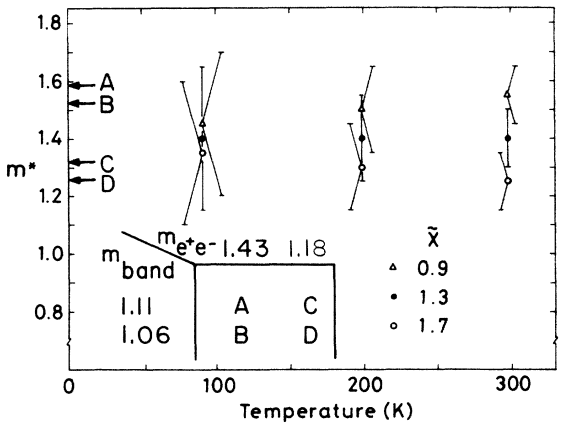

FIG. 7. Values of m^* obtained from fitting data at various temperatures keeping $\tilde{\chi}$ fixed. Requiring temperature independence leads to $\tilde{\chi}\approx 1.3$ and $m^*\approx 1.4m_e$. The theoretical values resulting from the various combinations of the band masses of $1.11m_e$ (Ref. 7) or $1.06m_e$ (Ref. 18) with the positron-electron mass enhancement factors of 1.18 (Ref. 9) or 1.43 (Ref. 11) are also indicated.

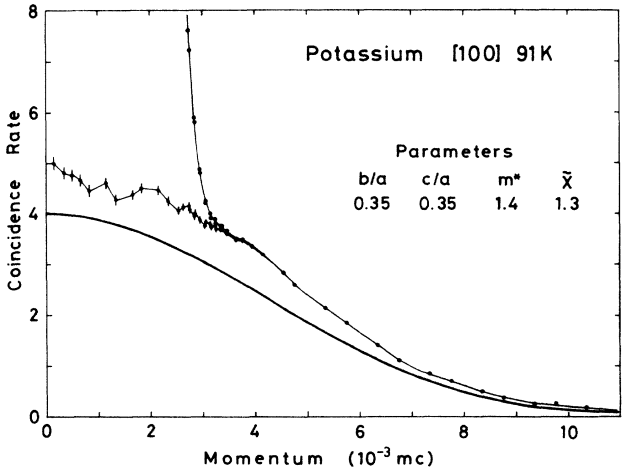

FIG. 8. An expanded portion of the data along [100] at 91 K, and the remainder after the parabolic part with the parameters determined by the analysis of the data along [110] has been subtracted. The assumed core contribution is the same as that in Figs. 3 and 5.

one estimated for the data at 298 K is shown in Fig. 6.

The shape of the sum of the argon-like core and the higher momentum components discussed above determines the "reasonableness" and consistency of the shape of the remainder obtained in subtracting the parabolic part from the data. In the actual procedure the best values for the Fermi momentum p_F and the parameters a, b/a, and c/a were searched for first, with the parameters for the positron momentum distribution tentatively fixed at some reasonable values. Some of the subtraction results are shown in Fig. 5, where the only parameter varied is the enhancement. The bars on the points indicate the errors resulting from the statistical errors of the whole angular correlation curve. Note that the component determined by curve (3) and the estimated core contribution (thick solid line) is similar to curves (1) and (2) for the higher momentum components in Fig. 4(b). In spite of the uncertainty in the core and higher momentum component contributions, the value of the enhancement is surprisingly constrained. The best values of enhancement at different temperatures were $b/a=c/a=0.3$–0.4 and are affected very little by the subsequent adjustment of other parameters. (We have put the constraint $b/a=c/a$ in the search because different pairs, as long as the sum $b/a+c/a$ is constant, give almost indistinguishable results.) The parameter a is related to the enhancement of the total annihilation rate of conduction electrons. However, it is meaningful as such only when we have a reliable independent-particle calculation of the angular correlation curve as well as a good estimate of the core enhancement factor. Thus a is regarded here as a parameter which determines the relative weight of the parabolic part. In practice, the portion of the parabolic part at $p=0$ was used to fix a. Then, with the above parameters fixed, the best values for the parameters $\tilde{\chi}$ and m^* in the positron momentum distribution (11) were searched for. Note that Gaussian distributions are included in this expression as the limit $\tilde{\chi}\to 0$. Several trials with only m^* varied are shown in Fig. 6.

The whole procedure was repeated a few times until a stable set of values of all the parameters was obtained. It was observed that different pairs of values of $\tilde{\chi}, m^*$ could give indistinguishable results. The parameters $\tilde{\chi}$ and m^* are, of course, temperature independent. Thus fitting data at several temperatures with $\tilde{\chi}$ fixed makes m^* appear to be a function of temperature unless $\tilde{\chi}$ is chosen correctly. The result of this procedure is shown in Fig. 7, from which we deduce $\tilde{\chi}\approx 1.3$ and $m^*\approx 1.4m_e$. The final results are shown in Table I.

To check the consistency of the analysis the parabolic part calculated with the parameters determined above is subtracted from the data along [100] at 91 K and shown

TABLE I. Results of analysis. p_F is the Fermi momentum, b/a and c/a are the parameters for the enhancement ($b/a=c/a$ is assumed), m^* the quasiparticle effective mass of the positron, and $\tilde{\chi}$ the renormalized positron-phonon coupling constant.

T (K)	p_F ($10^{-3}mc$)	$b/a(=c/a)$	m^*/m_e	$\tilde{\chi}$
91	2.87±0.02	0.40		
199	2.84±0.02	0.35	0.35±0.05	1.4±0.1	1.3±0.3
298	2.81±0.04	0.30		

in Fig. 8. The estimated core contribution is the same as that for the data along [110] at the same temperature (Fig. 5). The structure of the higher momentum component is similar to the prediction of the model calculation shown in Fig. 4.

V. DISCUSSION

In view of relatively large expansion coefficient ($\approx 8\times 10^{-5}$ K^{-1}) and low Debye temperature (≈ 100 K) of potassium, the temperature dependence of the high momentum portion of the angular correlation data shown in Fig. 3 is most likely due to the thermal expansion of the lattice and to the lattice vibrations. As has been discussed by Stott and West,[39] the volume expansion and the thermal vibrations will reduce the overlap of the positron wave function with the core electron wave functions, which results in a reduction of the intensity and probably the width of the core contribution. The intensity of the higher momentum components of the conduction-electron contribution is also expected to be reduced. Figure 3 shows these features qualitatively.

The momentum dependence of the enhancement of the annihilation rate observed in this work, Fig. 9, is not much different from the results of previous experiments with polycrystals.[5,14] There are several calculations on the momentum-dependent enhancement of the annihilation rate in the electron gas of different densities. Unfortunately, however, no calculation but Carbotte's[24] gives results close to that of potassium, $r_s=4.86$. Thus one is compelled to interpolate or extrapolate the existing results to estimate what the calculations predict. Among those calculations, Kahana's[23] and some of the extensions[24,25,27] of his formalism give results close to the present result, while a calculation by Boronski *et al.*[26] gives a larger momentum dependence. It is known,[28] however, that the total annihilation rate in the Kahana formalism diverges for $r_s > 6$ and so this agreement could be accidental. The calculation of Arponen and Pajanne[29] predicts a very small momentum dependence, especially for larger r_s. An interpolation of their result gives $b/a=0.1$ and $c/a=0.1$. Figure 5 includes the remainder after the parabolic part enhanced by these factors is subtracted. Despite their success in calculating the total annihilation rate,[1] it is apparent that their momentum dependence is too small to explain the experimental data. Although Lowy's result[30] gives a larger momentum dependence (roughly corresponding to $b/a=c/a=0.15$) than Arponen and Pajanne's, it is still about half the experimental value. Thus it appears that we do not have a theory yet which agrees with experiment both in the total annihilation rate and in the momentum dependence of the enhancement.

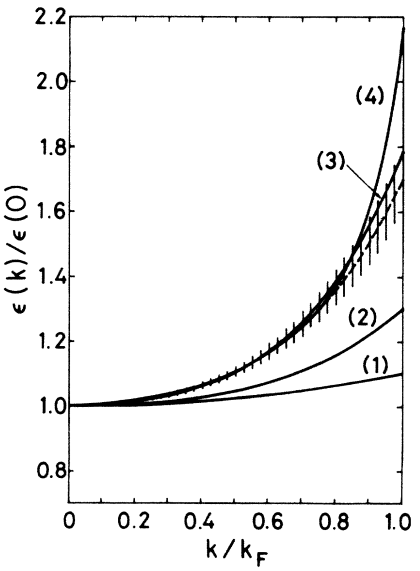

FIG. 9. The momentum dependence of enhancement, $\epsilon(k)$. Theoretical results are as follows: (1) Arponen and Pajanne (Ref. 29), (2) Lowy (Ref. 30), (3) Carbotte (Ref. 24), and (4) Boronski *et al.* (Ref. 26). Results from this experiment are shown as the dashed and shaded line.

The positron quasiparticle effective mass deduced in the present work, $m^*=(1.4\pm 0.1)m_e$ is certainly smaller than the apparent masses obtained in the previous experiments.[5,14] It is thus evident that these masses included the effect of the positron-phonon scattering, which has been extracted in the present work. Use of Stott and Kubica's band mass[7] of $m_b=1.11m_e$ and Hamann's[9] positron-electron mass enhancement factor of 1.18, calculated using the RPA, gives $m^*=\simeq 1.31m_e$. Baldo and Pucci's[11] positron-electron mass enhancement factor of 1.43 gives $m^*=\approx 1.59m_e$. The present experimental value 1.40 ± 0.10 lies between them. Use of the band mass of Fletcher *et al.*,[8] 1.06, gives similar results. Recently, Isii[40,41] has applied soliton theory to calculate the effective mass of positrons interacting with plasmons. Application of his result to real metals leads to much larger effective mass, of about $2.1m_e$ for potassium,[40,41,8] which is much larger than the experimental value obtained here.

The positron-phonon coupling constant χ given by (14) is readily estimated. For potassium $s_0=1.86$ km/s while an estimate using the bulk modulus gives $s=1.88$ km/s. Bergersen *et al.*[42] have estimated D for a number of metals and for potassium found $|3D/2E_F|=1.3$. Thus for potassium $\chi=1.7$. The present experimental result for $\chi=1.3\pm 0.3$ implies that $Z_0=0.76\pm 0.18$, close to Mori's[32] value for liquid state, 0.64, but a factor of 2 larger than the result of Baldo and Pucci,[11] $Z_0=0.38$.

VI. SUMMARY

The angular correlation of annihilation radiation from potassium single crystals has been measured to study the positron-electron and positron-phonon interactions. The data have been analyzed using a new procedure which is little affected by the uncertainty in the background consisting of the contributions from the core and higher momentum components of the wave functions. The momentum-dependent enhancement of the annihilation rate due to the positron-electron interaction has been shown to be larger than the results of recent theories which have succeeded in giving reasonable total annihilation rates. The existence of the long tail in the Fermi cut-

off smearing due to the tail in the positron momentum distribution has been confirmed. The true quasiparticle mass of positrons, free from phonon scattering effects, has been found to be $m^* = 1.4m_e$. The value of the renormalized positron-phonon coupling constant, $\tilde{\chi} = 1.3$, has also been obtained.

ACKNOWLEDGMENTS

This work was supported by the Natural Science and Engineering Research Council of Canada. One of the authors (T.H.) appreciates travel support provided by the Yoshida Foundations for Science and Technology.

*Present address: Institute of Physics, College of Arts and Sciences, University of Tokyo, 3-8-1 Komaba, Tokyo 153, Japan.

[1]J. Arponen and E. Pajanne, Ann. Phys. (N.Y.) **121**, 343 (1979).

[2]B. Bergersen and E. Pajanne, Phys. Rev. B **3**, 1588 (1971).

[3]A. T. Stewart and J. B. Shand, Phys. Rev. Lett. **16**, 261 (1966).

[4]A. T. Stewart, J. B. Shand, and S. M. Kim, Proc. Phys. Soc. **88**, 1001 (1966).

[5]S. M. Kim and A. T. Stewart, Phys. Rev. B **11**, 2490 (1975).

[6]C. K. Majumdar, Phys. Rev. **149**, 406 (1966).

[7]M. J. Stott and P. Kubica, Phys. Rev. B **11**, 1 (1975).

[8]G. Fletcher, J. L. Fry, and P. C. Pattnaik, Phys. Rev. B **27**, 3987 (1983).

[9]D. R. Hamann, Phys. Rev. **146**, 277 (1966).

[10]B. Bergersen and E. Pajanne, Phys. Rev. **186**, 375 (1969).

[11]M. Baldo and R. Pucci, Nuovo Cimento **23B**, 202 (1974).

[12]H.-J. Mikeska, Phys. Lett. **24A**, 402 (1967).

[13]H.-J. Mikeska, Z. Phys. **232**, 159 (1970).

[14]P. Kubica and A. T. Stewart, Can. J. Phys. **61**, 971 (1983).

[15]T. McMullen, T. Hyodo, and A. T. Stewart, in *Proceedings of the 6th Interantional Conference on Positron Annihilation,* edited by P. G. Coleman, S. C. Sharma, and L. M. Diana (North-Holland, Amsterdam, 1982), p. 204.

[16]T. Hyodo, T. McMullen, and A. T. Stewart, Can. J. Phys. **62**, 297 (1984).

[17]See, e.g., T. Hyodo, T. McMullen, and A. T. Stewart, in *Proceedings of the 6th International Conference on Positron Annihilation,* edited by P. G. Coleman, S. C. Sharma, and L. M. Diana (North-Holland, Amsterdam, 1982), p. 201, and references therein.

[18]Preliminary results were presented at the Sixth International Conference on Positron Annihilation; see Ref. 17.

[19]S. Berko, in *Positron Solid State Physics,* edited by W. Brandt and A. Dupasquier (North-Holland, Amsterdam, 1983).

[20]J. P. Carbotte and S. Kahana, Phys. Rev. **139**, A213 (1965).

[21]J. J. Donaghy and A. T. Stewart, Phys. Rev. **164**, 396 (1967).

[22]A fourth, variational, type of calculation was suggested by A. Hatano, H. Kanazawa, and Y. Mizuno, Prog. Theor. Phys. **34**, 875 (1965), but this approach has not been pursued further.

[23]S. Kahana, Phys. Rev. **129**, 1622 (1963).

[24]J. P. Carbotte, Phys. Rev. **155**, 197 (1967).

[25]J. Arponen and P. Jauho, Phys. Rev. **167**, 239 (1968).

[26]E. Boronski, Z. Szotek, and H. Stachowiak, Phys. Rev. B **23**, 1785 (1981).

[27]Z. Szotek, *Proceedings of the 6th International Conference on Positron Annihilation,* edited by P. G. Coleman, S. C. Sharma, and L. M. Diana (North-Holland, Amsterdam, 1982), p. 227.

[28]J. Crowell, V. E. Anderson, and R. H. Richie, Phys. Rev. **150**, 243 (1966).

[29]J. Arponen and E. Pajanne, J. Phys. F **9**, 2359 (1979).

[30]D. N. Lowy (now D. Neilson), Phys. Rev. B **26**, 60 (1982).

[31]V. L. Moruzzi, J. F. Janak, and A. R. Williams, *Calculated Electronic Properties of Metals* (Pergamon, New York, 1978).

[32]G. Mori, J. Phys. F **4**, 821 (1974).

[33]A. L. Fetter and J. D. Walecka, *Quantum Theory of Many-Particle Systems* (McGraw-Hill, New York, 1971).

[34]T. McMullen, J. Phys. F **6**, L323 (1976).

[35]W. A. Harrison, *Solid State Theory* (McGraw-Hill, New York, 1970), pp. 433 and 434.

[36]A. Perkins and J. P. Carbotte, Phys. Rev. B **1**, 101 (1970).

[37]T. McMullen, J. Phys. F **7**, 2041 (1977).

[38]L. Oberli, A. A. Manuel, R. Sachot, P. Descouts, M. Peter, L. P. L. M. Rabou, P. E. Mijnarends, T. Hyodo, and A. T. Stewart, Phys. Rev. B **31**, 1147 (1985).

[39]M. J. Stott and R. N. West, J. Phys. F **8**, 635 (1978).

[40]A. Isii, Phys. Lett. **88A**, 417 (1982).

[41]A. Isii, Prog. Theor. Phys. **70**, 644 (1983).

[42]B. Bergersen, E. Pajanne, P. Kubica, M. J. Stott, and C. H. Hodges, Solid State Commun. **15**, 1377 (1974).